



# HHS Public Access

Author manuscript

*J Proteomics Bioinform.* Author manuscript; available in PMC 2015 September 12.

Published in final edited form as:

*J Proteomics Bioinform.* ; 7(10): 296–302. doi:10.4172/jpb.1000332.

## Heterogeneity of The CD90<sup>+</sup> Population in Different Stages of Hepatocarcinogenesis

Smathorn Thakolwiboon<sup>1,3</sup>, Jianhui Zhu<sup>1</sup>, Qixing Liang<sup>2</sup>, Theodore H Welling<sup>1</sup>, Min Zhang<sup>2</sup>, and David M Lubman<sup>1,\*</sup>

<sup>1</sup>Department of Surgery, University of Michigan Medical Center, Ann Arbor, Michigan 48109, United States <sup>2</sup>Department of Biostatistics, University of Michigan School of Public Health, Ann Arbor, Michigan 48109, United States <sup>3</sup>Department of Medicine, Faculty of Medicine Siriraj hospital, Mahidol University, Bangkok10700, Thailand

### Abstract

We have characterized herein the heterogeneity of the CD90<sup>+</sup> population at each stage of hepatocarcinogenesis using a computer-assisted immunohistochemical staining evaluation method for quantitative analysis on tissue microarrays. We found that CD90 in Hepatocellular carcinoma (HCC) tissues, which has been shown to be a marker for cancer stem cells, is expressed on tumor cells, in the stroma or on endothelial cells. Sub-classification of the CD90<sup>+</sup> population was based on morphology and co-expression with known markers including CD45 and CD31. Multiple linear regression suggested that the percentage of CD90<sup>+</sup> cancer cells/hepatocyte ( $p < 0.0001$ ), level of overall CD90 expression ( $p < 0.0014$ ), and level of CD90 expression in tumor islands ( $p < 0.0001$ ) increased significantly in each stage of liver disease progression, while the level of stromal CD90 expression ( $p = 0.1129$ ) did not change significantly. Additionally, only the CD90<sup>+</sup> cancer cells were positive for other cancer stem cell (CSC) markers including CD24, CD44 and CD133 whereas the other CD90<sup>+</sup> cells were negative for these markers. CD90 expression in cirrhosis was observed in hepatocytes, the portal tract area and fibrous septa while CD90 expression in normal liver was limited only to the portal tract area. This study demonstrates the heterogeneity of the CD90<sup>+</sup> population in HCC where a small population of the CD90<sup>+</sup> cells that expressed other CSC markers are CSCs and are associated with advanced stages of hepatocarcinogenesis. This heterogeneity should be emphasized in further studies where other methods may not be able to discriminate these distinct types of CD90<sup>+</sup> cells.

Copyright: © 2014 Thakolwiboon S, et al.

This is an open-access article distributed under the terms of the Creative Commons Attribution License, which permits unrestricted use, distribution, and reproduction in any medium, provided the original author and source are credited

\***Corresponding author:** David M Lubman, Department of Surgery, University of Michigan Medical Center, 1150 West Medical Center Drive, Building MSRB1 Room A510B, Ann Arbor, MI, USA, 48109-0656, Tel: 734-647-8834; Fax: 724-615-2088; dmlubman@umich.edu.

**Citation:** Thakolwiboon S, Zhu J, Liang Q, Welling TH, Zhang M, et al. (2014) Heterogeneity of The CD90<sup>+</sup> Population in Different Stages of Hepatocarcinogenesis. *J Proteomics Bioinform* 7: 296-302. doi:10.4172/jpb.1000332

## Keywords

CD90; Thy-1; Cancer stem cell; Hepatocellular carcinoma; Hepatocarcinogenesis; Immunohistochemistry

---

## Introduction

Liver cancer is the third leading cause of cancer-related death around the world [1,2]. Annually, 780,000 cases are newly diagnosed and 750,000 people die from this deadly disease [1]. Although regular surveillance of patients is performed by a combination of imaging and serum  $\alpha$ -fetoprotein level, a large number of patients are diagnosed at an advanced stage [3]. Even after surgical resection, the long-term prognosis remains poor due to a high recurrence rate [4-6]. The treatment strategy for non-resectable or advanced HCC is palliative by using local regional therapies such as transarterial chemoembolization (TACE) or systemic chemotherapeutic agents. However, these approaches have limited efficacy [3]. Hence, novel therapeutic strategies and early detection are needed.

Hepatocellular carcinoma (HCC) is the most common primary liver cancer. It has been reported that the development of HCC is strongly related to cirrhosis of various etiologies, especially chronic hepatitis B and C infection, high alcohol consumption and nonalcoholic fatty liver disease (NAFLD) [7]. Recently, molecular pathways associated with HCC were identified, and novel therapeutic molecules have been developed [8,9]. However, the molecular and cellular basis of the disease progression is not fully understood.

The concept of cancer stem cells (CSCs) has been shown to provide an alternative explanation of disease progression, recurrence, and chemoresistance. Conceptually, CSCs are a subpopulation of cancer cells which can initiate and regenerate the tumor [10]. Recently, several groups of cells in HCC containing CD24<sup>+</sup> [11], CD44, CD90<sup>+</sup> [12] and CD133<sup>+</sup> [13-15] markers, were shown to be CSCs by xenograft transplant in immunodeficient mice (*in vivo*) and/or by performing sphere culture (*in vitro*). In particular, CD90 is considered as a candidate marker for several types of cancer including esophageal squamous cell carcinoma [16], lung cancer [17,18], gastric cancer [19], and glioma [20]. Moreover, CD90<sup>+</sup> cells in HCC were recently demonstrated to have CSC properties [12]. It has also been shown that overexpression of CD90 is associated with early recurrence, and poor survival in HCC [21,22]. However, CD90 expression has also been observed in stromal cells (e.g. mesenchymal stem cells (MSC), cancer-associated fibroblasts (CAF), and endothelium) of various cancers, and plays an important role in disease progression [23-27].

Immunohistochemistry (IHC) is a widely used technique for studying expression of a particular protein. Traditionally, pathologists have visually scored IHC data by using a product of the percentage of stained cells times the estimated staining intensity (e.g., 1, 2, or 3; where 0 is no staining, 1 is weak staining, 2 is moderate staining and 3 is strong staining) [28]. Therefore, this method is semi-quantitative in nature. Additionally, it is fraught with problems due to subjectivity in interpretation. A computer-assisted method is therefore employed in this study. In order to obtain truly quantitative data, we used the software to

analyze the optical density (OD) of stained pixels since OD has a linear relationship with stain concentration [29].

In this work, CD90 expression was observed on various cell types. This finding was confirmed by double immunofluorescence (IF) staining with antibodies of known cellular markers including CD31 (endothelial cells) and CD45 (leukocytes) as well as other CSC markers (CD24, CD44 and CD133). To avoid the effect of cellular heterogeneity of the CD90<sup>+</sup> population where CD90<sup>+</sup> cancer cells were only a few percent of the total, we separately analyzed the expression of CD90 in each subpopulation, using a computer-assisted method with IHC-stained tissue microarrays (TMAs) which allows us to quantitatively observe the changes of CD90 in different stages of hepatocarcinogenesis in a large sample set and obtain quantitative data for further statistical analysis. The CD90<sup>+</sup> cancer cells/hepatocytes and the amount of CD90 on the tumor region increased markedly from normal or cirrhosis samples to early-stage HCC while the expression on stroma did not change in the same trend. This phenomenon might otherwise have been missed in whole tissue studies or flow sorting which do not distinguish the different types of CD90 cells.

## Materials and Methods

### Tissue specimens

The formalin-fixed paraffin-embedded tissue microarrays (TMAs), Cat no. T032, BC03117, and BC03119, were purchased from US Biomax Inc. (Rockville, MD). Tissue samples on these TMAs include 149 HCC, 22 intrahepatic cholangiocarcinoma, 1 hepatic malignant fibrohistocytoma (MFH), 1 hepatic angiosarcoma, 22 cirrhosis, and 17 normal liver tissue spots.

In addition to TMAs, 5 formalin-fixed paraffin-embedded HCC and paired adjacent normal tissue sections were obtained. The tissue sections were 2×2 cm and 5 µm in thickness. All cases had no previous treatment.

### Antibodies

Primary antibodies were rabbit monoclonal anti-human CD90 IgG, mouse monoclonal anti-human CD24 IgG, mouse monoclonal anti-human CD31 IgG, mouse monoclonal anti-human CD44 IgG, mouse monoclonal anti-human CD45 IgG (Cat no. ab92574, ab76514, ab6124, ab9498, and ab8216, abcam, Cambridge, MA), and mouse monoclonal anti-human CD133 IgG antibodies (Cat no. MAB4399, Milipore, Temecula, CA). These antibodies have been validated by western blot and IHC staining. All antibodies are recommended for IHC or IF according to the manufacturer's data sheets.

For IHC staining, goat polyclonal anti-rabbit IgG H and L or goat polyclonal anti-mouse IgG H and L (Cat no. ab6721 and ab6789, abcam, Cambridge, MA) was used as secondary antibody. These antibodies were conjugated with horseradish peroxidase (HRP). For immunofluorescence (IF) staining, secondary antibodies were DyLight<sup>®</sup>488 Goat anti-rabbit IgG antibody and DyLight<sup>®</sup>549 Horse anti-mouse IgG antibody (Cat no. DI-1488 and DI-2549, Vector laboratories, Burlingame, CA).

These antibodies were diluted prior to use by 2% Bovine serum albumin (BSA). The information and dilution ratio of antibodies is shown in Table S1.

### **Immunohistochemical (IHC) study**

The tissue slides were deparaffinized in xylene, and rehydrated in a series of descending concentration of ethanol (100% twice, 95%, and 75%, 5 minutes each). Antigen retrieval was performed using citrate buffer solution pH6.0 (Cat no. Q2446, Teknova, Hollister, CA) heated to 92-98°C for 15 min and then cooled to room temperature. Endogenous peroxidase activity was blocked by incubating the slides in 3% Hydrogen peroxide. The slides were blocked with 2% BSA for 1 h at room temperature and incubated with the diluted primary antibody overnight at 4°C. Then the HRP-conjugated secondary antibody was diluted and incubated with the slides for an hour. Immunoreactions were detected by diaminobenzidine (ImmPACT™ DAB Substrate kit, catalog no. SK-4105, Vector laboratories, Burlingame, CA). Hematoxylin counterstaining was performed for nucleus visualization. The slides were then soaked in 1% HCl for a few seconds in order to remove non-specific Hematoxylin staining. Between each step, the slides were washed with PBST for 5 min 3 times. Finally, the slides were dehydrated in ethanol and xylene, and then covered by a cover glass and mounting medium (CC/Mount™, catalog no. C9368, Sigma-Aldrich, MO) before further analysis. Blank and isotype control were performed as the negative control experiments.

### **Double immunofluorescence (IF) study**

After deparaffinization, rehydration, and antigen retrieval, the tissue slides were blocked with 2% BSA for 1 h at room temperature. The mixture of desired diluted primary antibodies was incubated with the slides overnight at 4°C. After overnight incubation, secondary antibodies were diluted, mixed and incubated with the slides for an hour. Nuclei visualization was done by incubating the specimens in the dark with DAPI. Tissue slides were washed with PBST 3 times between each step. The slides were dehydrated in ethanol and xylene prior to being covered with cover glasses and mounting medium.

### **Evaluation of CD90 immunohistochemical staining on tissue microarray**

The IHC-stained TMAs were examined using a Nikon Eclipse Ti-U microscope (Nikon, Melville, NY) and a software called “NIS elements AR 4.13.00 (64 bit)”. Three pictures of each tissue spot were captured at the resolution of 0.34 μm/pixel. Since the light passing through the microscope is unpredictably modified before image analysis, white balance was accomplished by the software mentioned above in order to make colors in the capture images consistent with colors observed by human eyes. Tumor and stromal regions were identified manually based on morphology. Necrotic areas were excluded. The threshold for positive staining was set and validated at R 95-172, G 65-152, B 28-107. The baseline value was obtained from the negative control slides which were not incubated by primary antibody. Since the OD has a linear relationship with stain concentration [29], the ratio between summation of the individual OD of each pixel and analyzed area (OD/ area) was used for quantification of the level of CD90 expression. A percentage of CD90<sup>+</sup> cancer cells/hepatocytes was manually counted in 3 non-overlapping, randomly selected 200x fields containing at least 1,000 cancer cells/hepatocytes in total.

## Evaluation of double immunofluorescence staining

The double IF-stained TMAs were examined under 200× and 400× fields by Nikon Eclipse Ti-U microscope (Nikon, Melville, NY). Co-expressions of CD90 with other cellular markers (CD24, CD31, CD45, and CD133) were observed. CD31 and CD45 were used for identification of endothelia and leukocytes respectively while CD24 and CD133 served as CSC markers. Additionally, percentages of CD90<sup>+</sup> cancer cells which expressed CD24 or CD133 were manually counted in 3 non-overlapping, randomly selected 200x fields containing at least 1,000 cancer cells in total.

## Statistical analysis

Patient characteristics (age, gender, onset of hepatitis, and histological grade) in each disease category were compared using Chi-square test for categorical variables and analysis of variance (ANOVA) for continuous variables to identify potential confounders. Both unadjusted analyses using ANOVA and adjusted analyses controlling for factors which are significantly different among disease categories were then performed to study changes during hepatocarcinogenesis in the percentage of CD90<sup>+</sup> cancer cells/hepatocytes and level of CD90 expression. Specifically, in adjusted analyses, potential confounders are included as covariates in multiple linear regression, where disease categories are modeled as a categorical variable similar to ANOVA, often referred to as an “analysis of covariance” (ANCOVA) model, or alternatively as ordinal (Normal, Cirrhosis, Early-stage HCC and Late-stage HCC are coded as 1 to 4) in order to study the trend of CD90 expression with the progression of disease. For simplicity, we refer to the latter as multiple linear regression and the former as ANCOVA. P-value<0.05 was accepted as statistically significant. The reason we treated the group as both categorical (in ANCOVA) and ordinal (in the linear regression) is that, by treating the group as categorical, we can only test whether outcomes are different by groups but cannot test the trend (namely, we do not know how they are different). However, by treating the group as ordinal, we can also test whether the outcome is increasing with the severity of the disease (normal, cirrhosis, early-stage HCC, late-stage HCC).

## Results

### CD90 expression in non-cancerous liver tissue

In normal liver, CD90 expression was limited to the portal tract area. CD90<sup>+</sup> mature hepatocyte was not detected (Figure 1A). In cirrhosis, the majority of expression was found in the portal zone and fibrous septa. Many inflammatory cells in fibrous septa also expressed CD90. Interestingly, the expression of CD90 was observed in the cytoplasm of hepatocytes in 14/21 (66.7%) cirrhotic tissues as well (Figure 1B).

### CD90 expression in liver cancers

In HCC tissues, CD90 expression was observed in cancer cells, in the stroma, and on endothelia (Figure 1C). The majority of CD90 expression was in stroma. On the tumor islands of HCC, the mean (S.E.) for the percentage of CD90<sup>+</sup>cancer cell population was 5.93

(0.32)% of cancer cells. In HCC cancer cells, CD90 is localized to the cell membrane and cytoplasm (Figure 2).

In intrahepatic cholangiocarcinoma, CD90 expression was observed only in stroma and endothelium, not on cancer cells (Figure S1A). The high cytoplasmic CD90 expression was observed in a few cancer cells of hepatic MFH, a rare malignant mesenchymal tumor, while the vast majority showed low CD90 expression (Figure S1B). CD90 was expressed only in the perivascular area of hepatic angiosarcoma. In other areas, no CD90 expression was detected (Figure S1C).

As a consequence of an immune response against tumor, leukocytes are recruited to the tumor stroma. Importantly, CD90 expression on the subpopulation of leukocytes has been reported [30,31]. Hence, the exclusion of leukocytes is necessary in order to identify the real CD90<sup>+</sup> stromal population. In this study, CD45 was used as a marker to identify the leukocyte population. Double IF staining of CD45 and CD90 showed CD45<sup>-</sup>/CD90<sup>+</sup> cells, indicating the presence of a non-leukocyte CD90<sup>+</sup> population in stroma (Figure 3A). The co-expressions of CD31 with CD90 in HCC, cholangiocarcinoma, and MFH were observed by double IF staining (Figure 3B). This confirmed that CD90 also is expressed on the tumor endothelium of these aforementioned tumors. In angiosarcoma, the sarcoma with vascular origin, co-expression was also observed only in the perivascular area.

### Changes of CD90 expression in stages of hepatocarcinogenesis

CD90 expression was quantified by 2 variables, the percentage of CD90<sup>+</sup> cancer cells/hepatocytes and the level of expression (OD/area). Since this work is focused on CD90 expression during hepatocarcinogenesis, non-HCC liver cancers were excluded from the analysis. Early- and late-stage HCC were defined by stage I-II, and stage III-IV according to the AJCC system [32]. Patient characteristics are described in Table 1. Age and gender were significantly different among disease categories; compared with other groups, the normal group is younger and has more females. Therefore, age and gender are adjusted in the adjusted analyses (ANCOVA and multiple linear regression).

We analyzed the differences in the percentage of CD90<sup>+</sup> cancer cells/hepatocytes, level (OD/area) of overall CD90 expression as well as the level of expression in the tumor and stromal areas separately among disease categories of hepatocarcinogenesis. Boxplots of CD90 expression, as well as *p*-values, are displayed in Figure 4. An abrupt increase of the percentages of CD90<sup>+</sup> cancer cells/hepatocytes (Figure 4A) and CD90 expression in the tumor region (Figure 4B) were observed between cirrhosis and early-stage HCC while the changes between early- and late-stage HCC were relatively small. ANOVA and ANCOVA adjusted for age and gender show that there are statistically significant differences in CD90 expression, namely, percentage of CD90<sup>+</sup> cancer cells/hepatocytes, the level of overall CD90 expression, the level of expression in tumor cells during development of HCC, and the level of CD90 expression in the stroma, among disease categories. Besides Boxplot values of raw means and medians are also shown in Tables S2A-D for each disease category. Since differences in raw group-specific means are possibly due to differences in confounders, Tables S2A-D further show least square means controlling for differences in age and gender among groups, estimated from ANCOVA, and specifically the least square

means are the estimated mean for each group fixing age and gender proportion at the overall average. In addition, multiple linear regression treating the disease category as an ordinal variable revealed a significant increase in the percentage of CD90<sup>+</sup> cancer cells/hepatocytes, the level of overall CD90 expression, and the level of expression in tumor cells during development of HCC. Interestingly although CD90<sup>+</sup> stromal cells are the majority of CD90<sup>+</sup> population, the increase in the level of CD90 expression in the stroma as the disease progresses was not statistically significant, although differences among disease categories were found. We also tested group difference for various outcomes using the nonparametric Kruskal-Wallis Test, and the results were qualitatively the same as those using ANOVA but more statistically significant.

### Co-expression between CD90 and other cancer stem cell markers

IHC staining to recognize the expression pattern of CD24, CD44 and CD133 was also performed. The immunoreactivities of CD24, CD44 and CD133 were observed predominantly in the cytoplasm of cancer cells (Figure S2). In order to examine the co-expression between CD90 and other cancer stem cell markers, double IF studies were conducted. The mean (S.E.) for CD90<sup>+</sup> cancer cells that expressed CD133 was only 5.11 (1.8)%, while CD24 and CD44 were expressed by the majority 88.9 (4.4)% and 92.7 (4.6)% of CD90<sup>+</sup> cancer cells, respectively (Figure 5). No co-expression of CD90 and CD24, CD44 or CD133 was observed in the stromal population as well as normal liver or normal adjacent tissue.

### Discussion

CD90 is a 25-37 kDa GPI-anchored protein that maps to human chromosome 11q22.3. Expression of CD90 has been observed in various cell types and diseases. For each cell type and disease, it has different functions and is involved in various signaling pathways [33]. CD90<sup>+</sup> cells from HCC cell lines, tumor specimens, and blood samples have been functionally proven to be enriched for CSCs [12]. However, subsequent studies in cell lines and patient's specimens using CD90<sup>+</sup> cells from fluorescent-activated cell sorting (FACS) exhibited mesenchymal phenotypes, and its role in tumorigenicity was not consistently demonstrated in different cell lines [34,35].

This study has demonstrated the heterogeneity of the CD90<sup>+</sup> population in HCC where CD90 was found on the tumor, stromal or endothelial cells, and the majority of CD90<sup>+</sup> cells are in stroma. However, the significant increase of CD90 expression in advanced stages of hepatocarcinogenesis was found in the tumor component, not the stroma as shown in Figure 4. This may explain the inconsistency of tumor initiation capacity in different cell lines where CD90<sup>+</sup> phenotype was described as mesenchymal cells when using FACS for cell isolation as mentioned above. While the majority of CD90<sup>+</sup> cells were stromal cells, a small fraction were cancer cells, and some endothelia also expressed CD90.

As a result of host response to the tumor, lymphocytes that may express cell surface protein CD90 are recruited to tumor stroma. An anti-CD45 antibody that reacts with all isoforms in all nucleated cells of the haemopoietic lineage [36] was used to demonstrate the existence of CD45<sup>-</sup>/CD90<sup>+</sup> stromal cells. These CD45<sup>-</sup>/CD90<sup>+</sup> cells, as detected in the stroma of HCC

were identified as the genuine stromal cells. This subpopulation may include CAFs and MSCs as demonstrated in prostate cancer [37,38].

Similar to an earlier report [39], we did not detect CD90 expression on quiescent endothelium. Only some endothelia in cirrhosis, and HCC expressed CD90. Under non-physiological conditions, CD90 expression on endothelium is associated with pathological angiogenesis, involving the interaction with proinflammatory or cancer cells, and is related to cancer metastasis [39-42].

CD90 expression in cirrhosis was observed in a small percentage of hepatocytes, and fibrous septa. The characteristics of CD90<sup>+</sup> hepatocytes in cirrhosis have not been explored. According to a model of CSC evolution [10], these cells could possibly be pre-malignant neoplastic stem cells. Interestingly, CAF properties were found in multipotent adult stem cells, which also express CD90, from both HCC, and cirrhosis [43]. These findings suggest that the CD90 molecule in cirrhosis plays a crucial role in oncogenesis of HCC. In normal liver, we found CD90<sup>+</sup> cells in the portal tract area. This population is known to include hepatic progenitor cells [44].

In order to quantify the expression of CD90 in various components of tissue, we used a computer-assisted strategy to evaluate the IHC staining on TMAs. The level of expression was measured by the OD/ area ratio. Since OD has a linear relationship with stain concentration [29], the OD/area ratio represented the amount of CD90 in a particular area or CD90 expression density. This approach can quantitatively compare the expression of a protein of interest which is expressed in different regions of the tissue without the need to isolate the population of interest or perform protein extraction. This allows us to avoid erroneous results from mixed populations which is a common pitfall in proteomic studies.

Our results demonstrate the increase in overall CD90 expression in advanced stages of hepatocarcinogenesis which is consistent with the finding from an mRNA study of whole tissues [26]. However, this study did not study CD90 expression in different cell types. Because CD90 is expressed on various cell types, it is crucially important to identify the specific subpopulation that has a significant impact on disease. Hence, we explored CD90 expression by separately analyzing the expression on tumor and stromal components. While the CD90 expression on stroma did not increase significantly, significant overexpression on the tumor islands and an increase in percentage of CD90<sup>+</sup> cancer cells/ hepatocytes were observed in later stages of hepatocarcinogenesis. These results indicate that only CD90<sup>+</sup> cancer cells are involved in tumor initiation. Also, the co-expression of CD90 with other CSC markers, CD24 and CD133, was only observed on cancer cells, not on other CD90<sup>+</sup> cell types. These findings suggest that only CD90<sup>+</sup> cancer cells serve as CSCs in HCC.

Although the percentage of CD90<sup>+</sup> cancer cells in our study showed a considerable difference when compared with a previous report using FACS [12], evidence from another IHC study [22] has indicated a result consistent with our work. This difference can be explained by the morphological heterogeneity of the CD90<sup>+</sup> population, which FACS is not able to distinguish.



Our results indicate that the co-expression of CD90 and CD133 in cancer cells was rare while most of CD90<sup>+</sup> cancer cells expressed CD44. This fact supports the hypothesis that CD44<sup>+</sup> and CD90<sup>+</sup> share the same cellular origin and CD133<sup>+</sup> CSCs originate from the pluripotent stem cells which have different origins from CD44<sup>+</sup> and CD90<sup>+</sup> [45]. We also found that the overlap between CD24 and CD90 was very high and specific to cancer cells. Since the CSC properties of the CD24<sup>+</sup> [11], CD44<sup>+</sup> and CD90<sup>+</sup> [12] population have been demonstrated in previous studies, the combination of CD90 with CD24 or CD44 could be used to enrich the CSC population in HCC.

A study in a mouse model demonstrated that CD24<sup>+</sup> cells in normal adult mouse liver were able to differentiate into hepatocytes [46]. This suggests that CD24<sup>+</sup> hepatic progenitor cells which were differentiated from CD90<sup>+</sup> pluripotent stem cells may be the origin of CD24<sup>+</sup>/CD90<sup>+</sup>CSCs. However, the biological connection of CD24 and CD90 in humans still requires further studies.

## Conclusion

This is the first study that points out the heterogeneity of CD90<sup>+</sup> population and their changes in different stages of hepatocarcinogenesis. By quantitative analysis using computer-assisted IHC evaluation, we discovered that only the CD90 expression on the tumor islands or liver parenchymal, instead of the stroma, undergoes a significant increase during disease progression. Additionally, only CD90<sup>+</sup> cancer cells expressed other CSC markers while other CD90<sup>+</sup> populations did not express these markers. This heterogeneity in the CD90<sup>+</sup> population should be emphasized in CSC isolation in future studies since the results can be confounded by a mixed population.

## Supplementary Material

Refer to Web version on PubMed Central for supplementary material.

## Acknowledgement

This work was supported by the National Cancer Institute under grant CA160254 (David M. Lubman) and partial supported from the National Institute of Health through grant R01GM49500 (David M. Lubman). We also would like to acknowledge grant support to Dr. Thakolwiboon from the Prince Mahidol Award Youth Program (PMAYP).

## References

1. Ferlay, J.; Soerjomataram, I.; Ervik, M.; Dikshit, R.; Eser, S., et al. GLOBOCAN 2012 v1.0, Cancer Incidence and Mortality Worldwide: IARC CancerBase No. 11. In 2013 ed. International Agency for Research on Cancer; Lyon, France: 2013.
2. Soerjomataram I, Lortet-Tieulent J, Parkin DM, Ferlay J, Mathers C, et al. Global burden of cancer in 2008: a systematic analysis of disability-adjusted life-years in 12 world regions. *Lancet*. 2012; 380:1840–1850. [PubMed: 23079588]
3. Genco C, Cabibbo G, Maida M, Brancatelli G, Galia M, et al. Treatment of hepatocellular carcinoma: present and future. *Expert Rev Anticancer Ther*. 2013; 13:469–479. [PubMed: 23560841]
4. Lim KC, Chow PK, Allen JC, Siddiqui FJ, Chan ES, et al. Systematic review of outcomes of liver resection for early hepatocellular carcinoma within the Milan criteria. *Br J Surg*. 2012; 99:1622–1629. [PubMed: 23023956]

5. EASL-EORTC clinical practice guidelines: management of hepatocellular carcinoma. *J Hepatol.* 2012; 56:908–943. [PubMed: 22424438]
6. Welker MW, Bechstein WO, Zeuzem S, Trojan J. Recurrent hepatocellular carcinoma after liver transplantation - an emerging clinical challenge. *Transpl Int.* 2013; 26:109–118. [PubMed: 22994652]
7. El-Serag HB. Hepatocellular carcinoma. *N Engl J Med.* 2011; 365:1118–1127. [PubMed: 21992124]
8. Roberts LR, Gores GJ. Hepatocellular carcinoma: molecular pathways and new therapeutic targets. *Semin Liver Dis.* 2005; 25:212–225. [PubMed: 15918149]
9. Olsen SK, Brown RS, Siegel AB. Hepatocellular carcinoma: review of current treatment with a focus on targeted molecular therapies. *Therap Adv Gastroenterol.* 2010; 3:55–66.
10. Valent P, Bonnet D, De Maria R, Lapidot T, Copland M, et al. Cancer stem cell definitions and terminology: the devil is in the details. *Nat Rev Cancer.* 2012; 12:767–775. [PubMed: 23051844]
11. Lee TK, Castilho A, Cheung VC, Tang KH, Ma S, et al. CD24(+) liver tumor-initiating cells drive self-renewal and tumor initiation through STAT3-mediated NANOG regulation. *Cell Stem Cell.* 2011; 9:50–63. [PubMed: 21726833]
12. Yang ZF, Ho DW, Ng MN, Lau CK, Yu WC, et al. Significance of CD90+ cancer stem cells in human liver cancer. *Cancer Cell.* 2008; 13:153–166. [PubMed: 18242515]
13. Ma S, Chan KW, Hu L, Lee TK, Wo JY, et al. Identification and characterization of tumorigenic liver cancer stem/progenitor cells. *Gastroenterology.* 2007; 132:2542–2556. [PubMed: 17570225]
14. Suetsugu A, Nagaki M, Aoki H, Motohashi T, Kunisada T, et al. Characterization of CD133+ hepatocellular carcinoma cells as cancer stem/progenitor cells. *Biochem Biophys Res Commun.* 2006; 351:820–824. [PubMed: 17097610]
15. Yin S, Li J, Hu C, Chen X, Yao M, et al. CD133 positive hepatocellular carcinoma cells possess high capacity for tumorigenicity. *Int J Cancer.* 2007; 120:1444–1450. [PubMed: 17205516]
16. Tang KH, Dai YD, Tong M, Chan YP, Kwan PS, et al. A CD90(+) tumor-initiating cell population with an aggressive signature and metastatic capacity in esophageal cancer. *Cancer Res.* 2013; 73:2322–2332. [PubMed: 23382045]
17. Wang P, Gao Q, Suo Z, Munthe E, Solberg S, et al. Identification and characterization of cells with cancer stem cell properties in human primary lung cancer cell lines. *PLoS One.* 2013; 8:57020.
18. Yan X, Luo H, Zhou X, Zhu B, Wang Y, et al. Identification of CD90 as a marker for lung cancer stem cells in A549 and H446 cell lines. *Oncol Rep.* 2013; 30:2733–2740. [PubMed: 24101104]
19. Jiang J, Zhang Y, Chuai S, Wang Z, Zheng D, et al. Trastuzumab (herceptin) targets gastric cancer stem cells characterized by CD90 phenotype. *Oncogene.* 2012; 31:671–682. [PubMed: 21743497]
20. He J, Liu Y, Zhu T, Zhu J, Dimeco F, et al. CD90 is identified as a candidate marker for cancer stem cells in primary high-grade gliomas using tissue microarrays. *Mol Cell Proteomics.* 2012; 11:M111.
21. Lu JW, Chang JG, Yeh KT, Chen RM, Tsai JJ, et al. Overexpression of Thy1/CD90 in human hepatocellular carcinoma is associated with HBV infection and poor prognosis. *Acta Histochem.* 2011; 113:833–838. [PubMed: 21272924]
22. Guo Z, Li LQ, Jiang JH, Ou C, Zeng LX, et al. Cancer stem cell markers correlate with early recurrence and survival in hepatocellular carcinoma. *World J Gastroenterol.* 2014; 20:2098–2106. [PubMed: 24616575]
23. Mesri M, Birse C, Heidbrink J, McKinnon K, Brand E, et al. Identification and characterization of angiogenesis targets through proteomic profiling of endothelial cells in human cancer tissues. *PLoS One.* 2013; 8:78885.
24. Samaniego R, Estechea A, Relloso M, Longo N, Escat JL, et al. Mesenchymal contribution to recruitment, infiltration, and positioning of leukocytes in human melanoma tissues. *J Invest Dermatol.* 2013; 133:2255–2264. [PubMed: 23446986]
25. Schubert K, Gutknecht D, Köberle M, Anderegg U, Saalbach A. Melanoma cells use Thy-1 (CD90) on endothelial cells for metastasis formation. *Am J Pathol.* 2013; 182:266–276. [PubMed: 23159525]
26. Sukowati CH, Anfuso B, Torre G, Francalanci P, Crocè LS, et al. The expression of CD90/Thy-1 in hepatocellular carcinoma: an *in vivo* and *in vitro* study. *PLoS One.* 2013; 8:76830.

27. Kim YG, Jeon S, Sin GY, Shim JK, Kim BK, et al. Existence of glioma stroma mesenchymal stemlike cells in Korean glioma specimens. *Childs Nerv Syst.* 2013; 29:549–563. [PubMed: 23274635]
28. Ben Hamida A, Labidi IS, Mrad K, Charafe-Jauffret E, Ben Arab S, et al. Markers of subtypes in inflammatory breast cancer studied by immunohistochemistry: prominent expression of P-cadherin. *BMC Cancer.* 2008; 8:28. [PubMed: 18230143]
29. Ruifrok AC, Johnston DA. Quantification of histochemical staining by color deconvolution. *Anal Quant Cytol Histol.* 2001; 23:291–299. [PubMed: 11531144]
30. Ritter MA, Sauvage CA, Delia D. Human Thy-1 antigen: cell surface expression on early T and B lymphocytes. *Immunology.* 1983; 49:555–564. [PubMed: 6134665]
31. Guillot-Delost M, Le Gouvello S, Mesel-Lemoine M, Cheraï M, Baillou C, et al. Human CD90 identifies Th17/Tc17 T cell subsets that are depleted in HIV-infected patients. *J Immunol.* 2012; 188:981–991. [PubMed: 22184726]
32. Edge, S.; Byrd, DR.; Compton, CC.; Fritz, AG.; Greene, FL., et al. 7. American Joint Committee on Cancer; Chicago: 2010. *AJCC Cancer Staging Handbook.*
33. Rege TA, Hagood JS. Thy-1 as a regulator of cell-cell and cell-matrix interactions in axon regeneration, apoptosis, adhesion, migration, cancer and fibrosis. *FASEB J.* 2006; 20:1045–1054. [PubMed: 16770003]
34. Ho DW, Yang ZF, Yi K, Lam CT, Ng MN, et al. Gene expression profiling of liver cancer stem cells by RNA-sequencing. *PLoS One.* 2012; 7:37159.
35. Yamashita T, Honda M, Nakamoto Y, Baba M, Nio K, et al. Discrete nature of EpCAM+ and CD90+ cancer stem cells in human hepatocellular carcinoma. *Hepatology.* 2013; 57:1484–1497. [PubMed: 23174907]
36. Altin JG, Sloan EK. The role of CD45 and CD45-associated molecules in T cell activation. *Immunol Cell Biol.* 1997; 75:430–445. [PubMed: 9429890]
37. Brennen WN, Chen S, Denmeade SR, Isaacs JT. Quantification of Mesenchymal Stem Cells (MSCs) at sites of human prostate cancer. *Oncotarget.* 2013; 4:106–117. [PubMed: 23362217]
38. True LD, Zhang H, Ye M, Huang CY, Nelson PS, et al. CD90/THY1 is overexpressed in prostate cancer-associated fibroblasts and could serve as a cancer biomarker. *Mod Pathol.* 2010; 23:1346–1356. [PubMed: 20562849]
39. Lee WS, Jain MK, Arkonac BM, Zhang D, Shaw SY, et al. Thy-, a novel marker for angiogenesis upregulated by inflammatory cytokines. *Circ Res.* 1998; 82:845–851. [PubMed: 9576104]
40. Saalbach A, Hildebrandt G, Hausteiner UF, Anderegg U. The Thy-1/Thy-1 ligand interaction is involved in binding of melanoma cells to activated Thy-1-positive microvascular endothelial cells. *Microvasc Res.* 2002; 64:86–93. [PubMed: 12074634]
41. Jurisic G, Iolyeva M, Proulx ST, Halin C, Detmar M. Thymus cell antigen 1 (Thy, CD90) is expressed by lymphatic vessels and mediates cell adhesion to lymphatic endothelium. *Exp Cell Res.* 2010; 316:2982–2992. [PubMed: 20599951]
42. Dudley AC. Tumor endothelial cells. *Cold Spring Harb Perspect Med.* 2012; 2:a006536. [PubMed: 22393533]
43. Cesselli D, Beltrami AP, Poz A, Marzotto S, Comisso E, et al. Role of tumor associated fibroblasts in human liver regeneration, cirrhosis, and cancer. *Int J Hepatol.* 2011; 2011:120925. [PubMed: 22187657]
44. Weiss TS, Lichtenauer M, Kirchner S, Stock P, Aurich H, et al. Hepatic progenitor cells from adult human livers for cell transplantation. *Gut.* 2008; 57:1129–1138. [PubMed: 18417531]
45. Liu LL, Fu D, Ma Y, Shen XZ. The power and the promise of liver cancer stem cell markers. *Stem Cells Dev.* 2011; 20:2023–2030. [PubMed: 21651381]
46. Qiu Q, Hernandez JC, Dean AM, Rao PH, Darlington GJ. CD24-positive cells from normal adult mouse liver are hepatocyte progenitor cells. *Stem Cells Dev.* 2011; 20:2177–2188. [PubMed: 21361791]

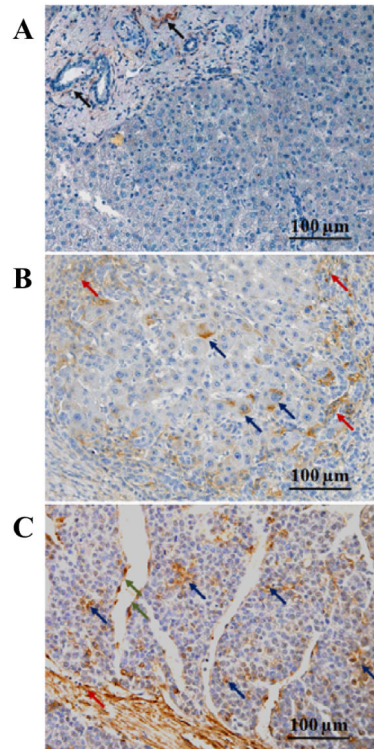


**Figure 1. CD90 expression in liver disease spectrum**

(A) Normal liver. Arrows indicate CD90 expression in portal area. Mature hepatocytes do not express CD90 protein.

(B) Chronic hepatitis with cirrhosis. Red arrows indicated CD90<sup>+</sup> population in fibrous septa which was infiltrated by inflammatory cells. Blue arrows indicated CD90<sup>+</sup> hepatocytes.

(C) Hepatocellular carcinoma. Red arrows indicated CD90 expression in tumor stroma. CD90<sup>+</sup> neoplastic cells were indicated by blue arrows. Green arrows indicate CD90<sup>+</sup> endothelium.

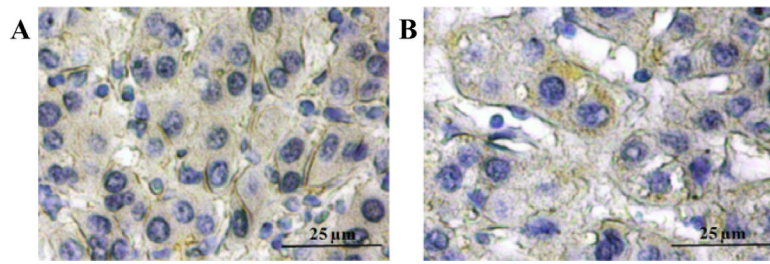


**Figure 2. Expression pattern of CD90 in neoplastic cells of hepatocellular carcinoma**  
Membranous (A) and cytoplasmic (B) expressions in neoplastic cells were demonstrated by immunohistochemical staining.

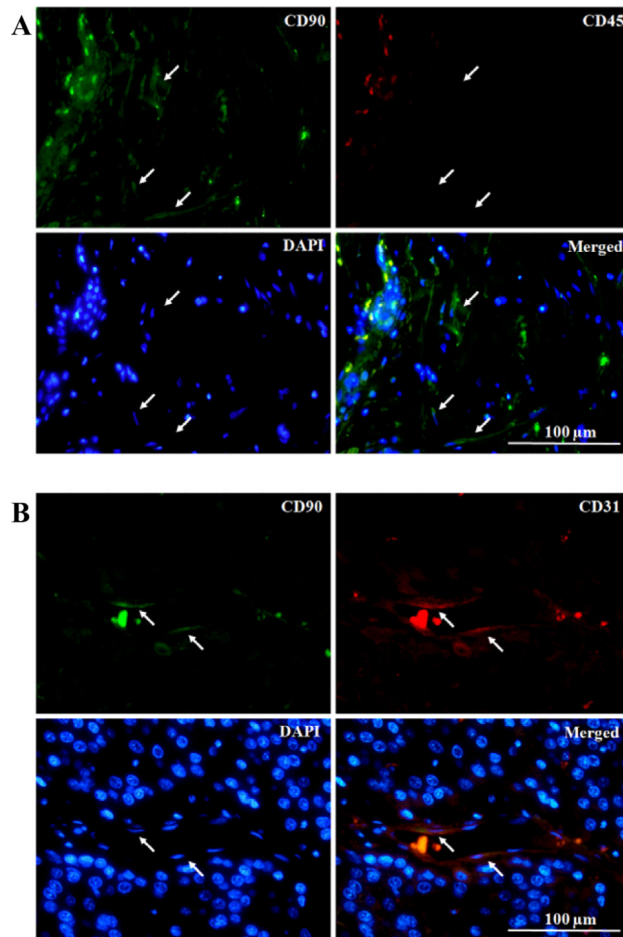


**Figure 3. CD90<sup>+</sup> stromal populations in hepatocellular carcinoma**

(A) Co-immunofluorescence staining showed the presence of non-leukocyte (CD45<sup>-</sup>) CD90<sup>+</sup> stromal population. CD90 (green), CD45 (red), and nucleus (blue). Arrows indicate CD45<sup>-</sup>/CD90<sup>+</sup> cells.

(B) The co-expression of CD90 and CD31 (endothelial marker). CD90 (green), CD31 (red), and nucleus (blue). Arrows indicate their co-expression on endothelium.

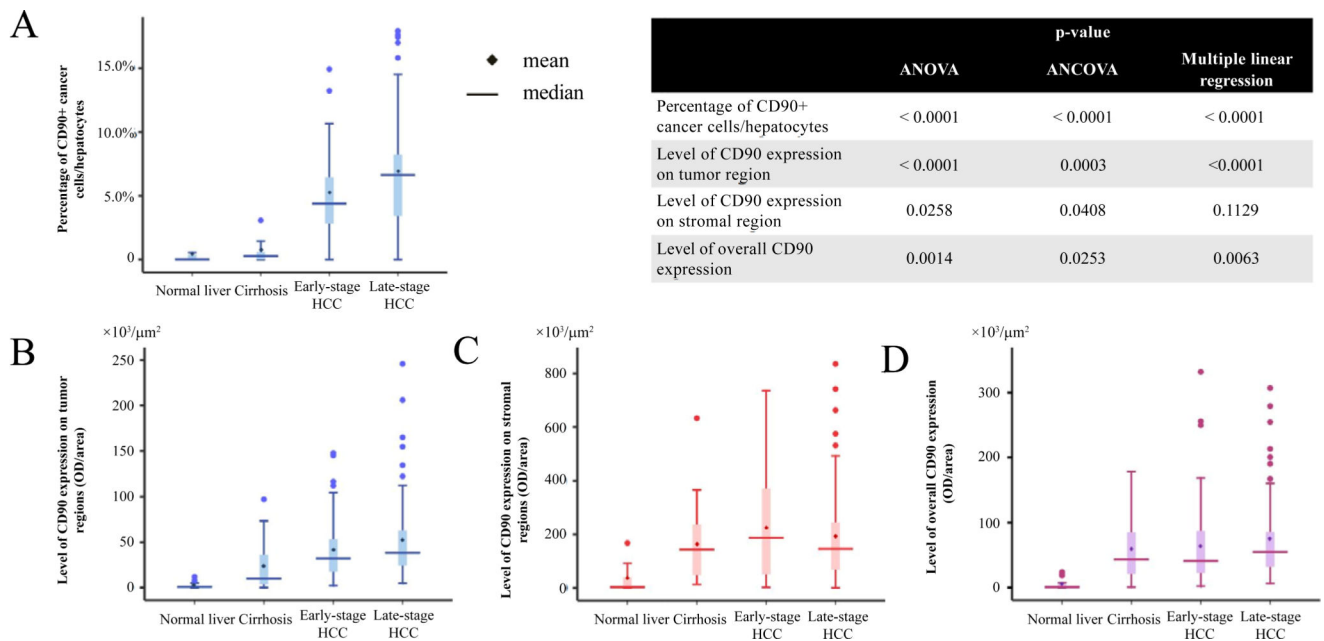


**Figure 4. Boxplots represent changes of CD90 expression during hepatocarcinogenesis** (A) Percentage of CD90 cancer cells/hepatocytes, (B) level of CD90 expression in tumor region, and (D) level of overall expression increased significantly during disease progression.

(C) Though levels of CD90 expression in stroma were significantly different among different disease categories, they did not show an increasing trend during hepatocarcinogenesis.

(Normal n=15, Cirrhosis n=21, Early-stage HCC n=67, Late-stage HCC n=82)

Inserted table: ‘multiple linear regression’ refers to the analysis where the group is treated as an ordinal variable; ‘ANCOVA’ (analysis of covariance) refers to the adjusted analysis where the group is treated as categorical variable.

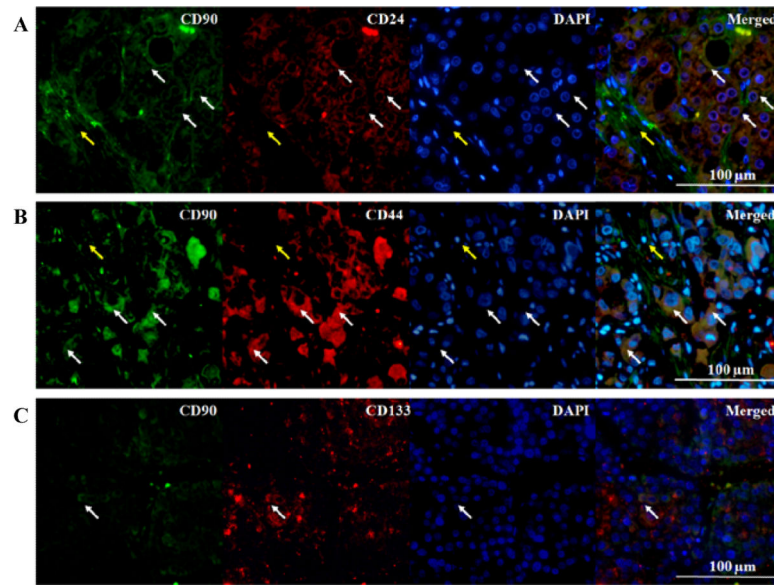


**Figure 5. Co-expression of CD90 and other neoplastic stem cell markers in hepatocellular carcinoma**

(A, B) Co-expression with CD24 and CD44 was observed in a majority of CD90<sup>+</sup> neoplastic cells. CD90 (green), CD24 or CD44 (red), and nucleus (blue). White arrows indicated examples of CD24<sup>+</sup>/CD90<sup>+</sup> cells. Yellow arrows showed that CD90<sup>+</sup> stromal cells did not express CD24 or CD44.

(C) The co-expression of CD90 and CD133 was rarely observed. CD90 (green), CD31 (red), and nucleus (blue). Arrows indicated their co-expression on neoplastic cells.



**Table 1**

Case characteristics \*

	Normal (n=15)	Cirrhosis (n=21)	Early-stage HCC (n=67)	Late-stage HCC (n=82)	p-value
Age (yr)	28.5 ± 14.1	50.7 ± 8.7	51.2 ± 9.2	51.0 ± 12.5	<0.0001 <sup>†a</sup>
Gender					
M	8	19	56	67	0.0289 <sup>†b</sup>
F	7	2	11	15	
Onset of hepatitis (yr)		16.3 ± 11.7	13.1 ± 9.4	16.0 ± 10.8	0.6054 <sup>a</sup>
Histological grade					
Grade 1			6	8	0.0830 <sup>b</sup>
Grade 2			46	49	
Grade 3			8	20	
Grade 4			0	0	

\* Plus-minus differences are mean ± SD

<sup>†</sup>  $p < 0.05$ <sup>a</sup>  $p$ -value by ANOVA<sup>b</sup>  $p$ -value by chi-square test